Quantum Information Processing (2019) 18:204
https://doi.org/10.1007/s11128-019-2320-8

Process estimation in qubit systems: a quantum decision theory approach

Ivan Maffeis[1] · Seid Koudia[2] · Abdelhakim Gharbi[2] · Matteo G. A. Paris[1]

Received: 7 December 2018 / Accepted: 9 May 2019

Abstract
We address quantum decision theory as a convenient framework to analyse process discrimination and estimation in qubit systems. In particular, we discuss the following problems: (1) how to discriminate whether or not a given *unitary perturbation* has been applied to a qubit system; (2) how to determine the amplitude of the *minimum detectable perturbation*. In order to solve the first problem, we exploit the so-called Bayes strategy and look for the optimal measurement to discriminate, with minimum error probability, whether or not the unitary transformation has been applied to a given signal. Concerning the second problem, the strategy of Neyman and Pearson is used to determine the ultimate bound posed by quantum mechanics to the minimum detectable amplitude of the qubit transformation. We consider both pure and mixed initial preparations of the qubit and solve the corresponding binary decision problems. We also analyse the use of entangled qubits in the estimation protocol and found that entanglement, in general, improves stability rather than precision. Finally, we take into account the possible occurrence of different kinds of background noise and evaluate the corresponding effects on the discrimination strategies.

Keywords Quantum decision theory · Quantum hypothesis testing · Process discrimination · Qubit interferometry

1 Introduction

The existence of non-orthogonal quantum states is one of the fundamental traits of quantum mechanics and has profound implications on its applications. On the one

✉ Matteo G. A. Paris
matteo.paris@fisica.unimi.it

[1] Quantum Technology Lab, Dipartimento di Fisica Aldo Pontremoli, Università degli Studi di Milano, 20133 Milan, Italy

[2] Laboratoire de Physique Théorique, Faculté des Sciences Exacte, Université de Bejaia, 06000 Bejaïa, Algeria

Published online: 16 May 2019

hand, non-orthogonality poses limitations to the fundamental challenge of quantum state discrimination [1–14] and, on the other hand, it may be exploited as a resource in quantum technologies, e.g. in quantum cryptography [15–27]. Non-orthogonality also influences other fundamental tasks in quantum information processing, and in particular process discrimination [28–36], which itself represents a crucial ingredient for quantum simulations and quantum interferometry [37–39].

In this paper, we address process discrimination in qubit systems and exploit results from quantum decision theory in order to optimise the discrimination strategy [40,41], i.e. to minimise the impact of non-orthogonality, and to derive the corresponding ultimate bounds to the *probability of error* in the detection of the perturbation, and the *discrimination precision* of the perturbation amplitude. The possible advantages resulting from the use of entanglement are also explored in details.

The scheme we are going to consider is the following: a single- or two-qubit system is prepared in a given initial state, then, with a certain unknown probability, it is subjected to the action of a given unitary operator $U_\lambda = \exp\{-iG\lambda\}$, G being the *generator* of the perturbation and λ its *amplitude*. Finally, the system is measured, in order to detect whether or not the unitary transformation has perturbed the system. The problem is equivalent to that of discriminating the unperturbed state of the system from the perturbed one, while accepting a probability of error. A second, complementary, goal is to determine the minimum detectable value of the amplitude λ which leads to discriminable outputs. The precision obtained by using one- or two-qubit will be compared in order to reveal whether the use of entanglement leads to some advantages, either in ideal conditions or in the presence of noise.

The paper is structured as follows. In Sect. 2, we establish notation and briefly review few fundamental results in quantum discrimination theory, also illustrating the different figures of merit employed in the so-called *Bayes* and *Neyman–Pearson* discrimination strategies. In Sect. 3, we employ Bayes strategy to distinguish between different processes with minimum error using one- and two-qubit probes, also when different kind of noise occurs. In Sect. 4, we exploit Neyman–Pearson strategy to find the ultimate bound to the minimum detectable perturbation, discrimination, also addressing the use of entanglement and the occurrence of noise. Finally, Sect. 5 is closing the paper with some concluding remarks.

2 Quantum decision theory

Let us consider a qubit system and assume it may be prepared in one of the two states $\{\rho_j\}_{j=1,2}$ with prior probabilities $\{z_j\}_{j=1,2}$ such that $\rho_j \in \mathcal{L}(\mathbb{C}^2)$, and $\sum_j z_j = 1$. Our goal is that of inferring the state of the qubit, basing our decision on the outcome of a measurement performed on the system. To this aim, we should implement a detection scheme, i.e. a POVM (Positive Operator-Valued Measure) $\Pi = \{\Pi_k\}_{k=1,2}$, where the Π_k's are positive semi-definite, $\mathrm{Tr}[\rho\,\Pi_k] \geq 0, \forall\rho$, and sum to the identity $\sum_k \Pi_k = \mathbb{I}$.

As we already mentioned, we cannot, even in principle, perfectly distinguish the two states, unless they have orthogonal supports. For non-orthogonal states, we cannot achieve perfect discrimination. However, we may seek for an *optimal discrimination strategy*, which minimise/maximise, in average, a given loss/gain function. In the

following two paragraphs, we briefly review two relevant strategies used in quantum hypothesis testing, which will be also at the basis of our approach to process estimation in qubit systems.

The first paragraph is devoted to Bayes strategy, which aims to the POVM minimising the average probability of error in the decision process. Bayes strategy is suitable for those situations where the two possible outcomes of the measurement are equally important for the experimenter and thus the two error probabilities should be jointly minimised. The paradigmatic situation where the Bayes strategy is employed is binary quantum communication, in which two classical symbols are encoded onto quantum states of a physical system and quantum decision theory is exploited to determine the optimal receiver at the output of the communication channel.

On the other hand, there are several situations of interest where one of the two events, usually referred to the *alternative hypothesis*, is expected to occur more rarely with respect to the other one, called *null hypothesis*. In these cases, the detection of alternative hypothesis is the main task of the measurement. The so-called Neyman–Pearson (NP) strategy is relevant for this context, aiming at maximising the detection probability of the alternative hypothesis while accepting a possible *false-alarm probability*, which is the probability of inferring the alternative hypothesis when the null hypothesis is instead true. A possible paradigmatic situation where NP strategy may be successfully implemented is the interferometric detection of gravitational waves.

2.1 Bayes discrimination strategy

Bayes strategy aims at minimising the average probability of error of the decision process [11], i.e. the quantity

$$q_e(\Pi) = \sum_{i \neq j} z_j \; p\,(i\,|\,j)\,,$$

where $p\,(i\,|\,j) = \mathrm{Tr}\left[\rho_j \Pi_i\right]$ is the probability of inferring ρ_i when ρ_j is the actual state of the system. In turn, Bayes strategy is also referred to as *minimum error* discrimination strategy [25–27]. Since we are here considering binary decisions, the probability of error simplifies to

$$q_e(\Pi) = z_1 - \mathrm{Tr}\left[\Lambda\, \Pi_1\right] = z_0 + \mathrm{Tr}\left[\Lambda\, \Pi_0\right], \tag{1}$$

where

$$\Lambda = z_1 \rho_1 - z_0 \rho_0. \tag{2}$$

This operator is hermitian, though not positive definite. It is sometimes referred to as the *Bayesian characteristic operator*.

As we can see from (1), the probability of error is minimised when the measurement operator Π_1 is the projector on the positive part of Λ. It is thus a projective valued measure (PVM) given by $\Pi = \{\mathbb{I} - \Pi_1, \Pi_1\}$ where $\Pi_1 = \sum_{\lambda_k > 0} |\lambda_k\rangle\langle\lambda_k|$ and

$\{\lambda_k\}_{k=0,1}$ are the eigenvalues of Λ. The resulting minimum probability of error may be written as:

$$p_e \equiv \min_{\Pi} q_e(\Pi) = \frac{1}{2}(1 - \mathrm{Tr}|\Lambda|) = \frac{1}{2}(1 - \|z_1\rho_1 - z_0\rho_0\|_1), \tag{3}$$

where the trace norm $\|A\|_1$ of an operator is defined as $\|A\|_1 = \mathrm{Tr}|A| = \mathrm{Tr}[\sqrt{A^\dagger A}]$. The quantity p_e in Eq. (3) is usually referred to as the *Helstrom bound* to the error probability in binary state discrimination. For pure states the Helstrom bound may be rewritten as

$$p_e = \frac{1}{2}\left[1 - \sqrt{1 - 4z_0 z_1 |\kappa|^2}\right], \tag{4}$$

where $\kappa = \langle\psi_1|\psi_0\rangle$ is the overlap between the two states. We can easily see that for vanishing overlap the probability of error is also vanishing as $p_e \overset{|\kappa|\to 0}{\simeq} z_0 z_1 |\kappa|^2$, whereas for large κ ($\kappa \to 1$), the discrimination process approaches pure guessing ($p_e \to 1/2$).

2.2 Neyman–Pearson discrimination strategy

Neyman–Pearson strategy aims at maximising the detection probability of the alternative hypothesis, at a fixed value of the false-alarm probability. Let us refer to the two hypotheses $\{H_0, H_1\}$ as the null and the alternative hypothesis, respectively, where $H_{j,\, j=0,1}$ corresponds to the qubit being in the state ρ_j. The basis of NP strategy is in fact a trade-off between the probability of detection of alternative hypothesis, $p(1|1) \equiv p_{11}$, and the false-alarm probability, $p(1|0) \equiv p_{10}$. A maximum threshold of false-alarm probability is fixed as acceptable, given the nature of the physical problem where the decision strategy is implemented. The searching of the POVM maximising the detection probability p_{11} corresponds to a Lagrange maximisation problem where the value of p_{10} is taken as a constraint. The optimal POVM is then the one maximising the Lagrange functional [4]:

$$L = p_{11} - \gamma\, p_{10} = \mathrm{Tr}[\Gamma\, \Pi_1],$$

where γ is a Lagrange multiplier and

$$\Gamma = \rho_1 - \gamma\rho_0 \tag{5}$$

is the Lagrange operator. In order to maximise L, the POVM Π_1 needs to be a projector on the positive eigenvalues of the operator Γ. The optimal measurement scheme according to Neyman–Pearson strategy is thus a projective one $\Pi = \{\mathbb{I} - \Pi_1, \Pi_1\}$ where $\Pi_1 = \sum_{g>0} |g\rangle\langle g|$, g being the eigenvalues of Γ and $|g\rangle$ the corresponding eigenvectors. We notice that, in solving the eigenvalue problem, different values of γ correspond to different values of the accepted false-alarm probability and thus to different Neyman–Pearson strategies.

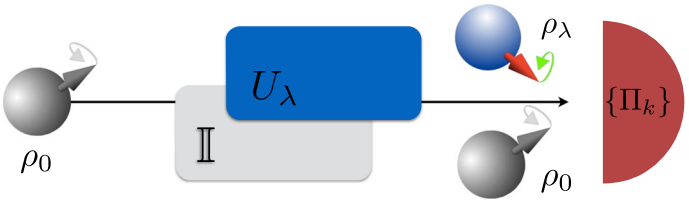

Fig. 1 Process discrimination as a binary decision problem. A single qubit initially prepared in the quantum state ρ_0 may, or may not, undergo a unitary transformation U_λ. A detector is placed at the output of the system to discriminate between the two states and, in turn, whether the unitary transformation has occurred or not

Once the eigenvalues of Γ are found, the strategy becomes clear: when the measurement of Γ gets a positive outcome, the alternative hypothesis H_1 is inferred as true, otherwise the null hypothesis H_0 is inferred. For pure states the detection probability p_{11} can be written in terms of p_{10} after eliminating the Lagrange multiplier γ, obtaining:

$$p_{11}\,(p_{10}) = \begin{cases} \left[\sqrt{p_{10}\,|\kappa|^2} + \sqrt{(1-p_{10})(1-|\kappa|^2)}\right]^2 & 0 \le p_{10} \le |\kappa|^2, \\ 1 & |\kappa|^2 < p_{10} \le 1. \end{cases} \tag{6}$$

Equation (6) shows that we may have unit detection probability as far as we accept a false-alarm probability larger than the overlap between the two pure states involved in the problem. As a consequence, as the overlap is large, the detection of the alternative hypothesis becomes hard, as either the detection probability cannot achieve the unit value without accepting extremely large margins of error (false alarm).

3 Bayes approach to process detection in qubit systems

3.1 Single-qubit states

In this section, we apply Bayes strategy to quantum binary discrimination to observe whether or not a given unitary perturbation has been applied to a qubit system. The detection scheme is schematically illustrated in Fig. 1.

A single-qubit system is initially prepared in an input quantum state ρ_0 and it is then let to evolve through a channel where it may undergo a transformation U_λ, being λ the perturbation amplitude. At the output, i.e .after the (possible) transformation we want to know whether we have ρ_0 or

$$\rho_\lambda = U_\lambda^\dagger \rho_0 U_\lambda \tag{7}$$

as output state. The problem reduces to discrimination between the two states, and since they do not have, in general, orthogonal supports, quantum decision theory is the natural framework to adopt. In the following, we will employ Bayes strategy for single-qubit signals, as well as two-qubit ones, in order to detect perturbations induced

by a Pauli matrix and, without loss of generality, we will assume

$$U_\lambda = e^{-i\lambda\sigma_1} = \cos\lambda\,\mathbb{I} - i\,\sin\lambda\,\sigma_1 \tag{8}$$

as the transformation which may take place into the channel. Upon writing the initial single-qubit state in a Bloch form $\rho_0 = \frac{1}{2}(\mathbb{I} + \mathbf{r}\cdot\boldsymbol{\sigma})$, with $\mathbf{r} = \{r_1, r_2, r_3\}$, $\boldsymbol{\sigma} = \{\sigma_1, \sigma_2, \sigma_3\}$, the transformed state is given by $\rho_\lambda = \frac{1}{2}(\mathbb{I}+\mathbf{r}_\lambda\cdot\boldsymbol{\sigma})$ where the transformed components are given by

$$\begin{aligned} r_{1\lambda} &= r_1, \\ r_{2\lambda} &= r_2\cos 2\lambda - r_3\sin 2\lambda, \\ r_{3\lambda} &= r_2\sin 2\lambda + r_3\cos 2\lambda. \end{aligned} \tag{9}$$

The characteristic operator in (2) becomes $\Lambda = \begin{pmatrix} \Lambda_0 & \Lambda_2 \\ \Lambda_2^* & \Lambda_1 \end{pmatrix}$, with:

$$\begin{aligned} \Lambda_0 &= z_1\,(1 + r_{3\lambda}) - z_0\,(1 + r_3)\,, \\ \Lambda_1 &= z_1\,(1 - r_{3\lambda}) - z_0\,(1 - r_3)\,, \\ \Lambda_2 &= z_1\,(r_{1\lambda} - i\,r_{2\lambda}) - z_0\,(r_1 - i\,r_2)\,. \end{aligned} \tag{10}$$

In this context, z_1 and z_0 are, respectively, the prior probabilities for the unitary transformation to have effect on the initial quantum state or not ($z_0 + z_1 = 1$). Upon evaluating explicitly trace and determinant of Λ, the probability of error has the following form:

$$p_e = \frac{1}{2}\left[1 - \sqrt{r^2 - 4z_1z_0\left[r^2 - \left(r^2 - r_1^2\right)\sin^2\lambda\right]}\right], \tag{11}$$

in which $r^2 = |\mathbf{r}|^2 = r_1^2 + r_2^2 + r_3^2$. If the state is pure, $r^2 = 1$, we indeed recover Eq. (4) since we have $|\kappa|^2 = 1 - (1 - r_1^2)\sin^2\lambda$. In the limiting cases where both eigenvalues are positive (negative) discrimination reduces to pure guessing, i.e. the inference is made without looking at data. We may summarise the situation as follows:

$$\begin{array}{ll} \mathrm{Tr}[\Lambda] \le 0 & Tr[\Lambda] > 0 \\ \Pi = \{\Pi_0 = \mathbb{I}, \Pi_1 = \mathbb{O}\} & \Pi = \{\Pi_0 = \mathbb{O}, \Pi_1 = \mathbb{I}\} \\ p_e = z_1 & p_e = z_0 \end{array} \tag{12}$$

Let us now assume $z_1 = z_0 = \frac{1}{2}$ (no *a priori* information about the occurrence of the perturbation) and rewrite (11) in terms of the initial state purity

$$p_e = \frac{1}{2}\left[1 - \sqrt{\left(2\mu - 1 - r_1^2\right)\sin^2\lambda}\right]. \tag{13}$$

The probability of error achieves its minimum when the input signal is pure ($\mu = 1$), and its projection on the direction of the generator vanishes, i.e. for pure states lying

in the orthogonal plane of the generator σ_1. In this case we have

$$p_e = \frac{1}{2}\left(1 - |\sin\lambda|\right) \tag{14}$$

which only depends on the parameter of the transformation. This is the least possible error we can get. Any discrimination procedure in the Bayesian sense is thus preparation dependent, at least for the present single-qubit case. We also note that all the above results generalise, *mutatis mutandis*, to any generator σ_k ($k = 1, 2, 3$).

3.2 Two-qubit states

Let us now consider the scheme in Fig. 2, where we assume that the qubit which may possibly subject to the transformation U_λ is initially prepared in an entangled state with another qubit.

Our goal is to compare the performance of this scheme against those if the single-qubit one at fixed use of the resource, here intended as the device that may impose the perturbation. Starting with a singlet state $|\psi_-\rangle = (|01\rangle - |10\rangle)/\sqrt{2}$, the density matrix of the corresponding perturbed state may be written as

$$\begin{aligned}\rho_\lambda = &\cos^2\lambda\,|\psi_-\rangle\langle\psi_-| + \sin^2\lambda\,|\phi_+\rangle\langle\phi_+| \\ &+ i\,\sin\lambda\cos\lambda\,\left(|\psi_-\rangle\langle\phi_-| - |\phi_-\rangle\langle\psi_-|\right),\end{aligned} \tag{15}$$

where the perturbation U_λ is acting on the first qubit in the singlet. The Bayesian characteristic operator is thus given by

$$\begin{aligned}\Lambda = &(z_1\cos^2\lambda - z_0)|\psi_-\rangle\langle\psi_-| + \sin^2\lambda\,|\phi_+\rangle\langle\phi_+| \\ &+ i\,\sin\lambda\,\cos\lambda\,\left(|\psi_-\rangle\langle\phi_-| - |\phi_-\rangle\langle\psi_-|\right),\end{aligned} \tag{16}$$

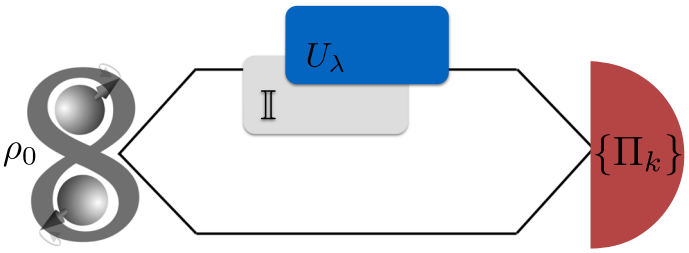

Fig. 2 Process discrimination as a binary decision on entangled state: the transformation U_λ that may or may not perturb the system, is acting on a qubit which is part of a bipartite system prepared in an entangled state. At the output, a joint detector is placed

and the corresponding eigenvalues by $\xi_{\pm} = \frac{1}{2}[(z_1 - z_0) \pm \sqrt{1 - 4z_0 z_1 \cos^2 \lambda}]$. The error probability reads as follows:

$$p_e = z_1 - \xi_+ = \frac{1}{2}\left[1 - \sqrt{1 - 4z_0 z_1 \cos^2 \lambda}\right]. \tag{17}$$

Using entanglement we may thus achieve the ultimate bound in Eq. (14) and, remarkably, the same results, i.e. the same value of p_e in Eq. (17) is obtained for any initial two-qubit preparation of the form

$$|\psi\rangle = \frac{1}{\sqrt{2}}\left[\alpha_0|00\rangle + \alpha_1|01\rangle + \alpha_2|10\rangle + \alpha_3|11\rangle\right], \tag{18}$$

provided that $\alpha_0\alpha_2^* + \alpha_1\alpha_3^* = 0$. In addition, under the same condition, Eq. (17) also holds when the perturbation is generated by any of the σ_k, $k = 1, 2, 3$. The class of states in Eq. (18) includes maximally entangled states. Upon comparing Eqs. (18) with (13), we see that entanglement improves the discrimination process in terms of *stability*, since the probability of error does not depend on the projection of the Bloch vector on the axis corresponding to the generator of the perturbation.

Let us now consider a generic mixture of Bell states:

$$\rho_0 = p_0|\phi_+\rangle\langle\phi_+| + p_1|\psi_+\rangle\langle\psi_+| + p_2|\psi_-\rangle\langle\psi_-| + p_3|\phi_-\rangle\langle\phi_-|.$$

After lengthy but straightforward calculation the characteristic operator can be obtained (not shown here) and, in turn, the following probability of error:

$$p_e = \frac{1}{2}[1 - (|p_0 - p_1| + |p_1 - p_3|)|\sin\lambda|]. \tag{19}$$

3.3 Bayes strategy in presence of noise

A possible generalisation of the problem is considering a situation where some source of noise acts during propagation of the signal. In particular, we focus on the two-qubit case, assuming that noise occurs to both parties and takes place before the possible perturbation U_λ. A schematic diagram of the experimental protocol is shown in Fig. 3. We present here the analysis of the effects on the same initial entangled state of four different kinds of noise: the three formalised by Pauli matrices and the depolarising noise.

The analysis here presented considers as first case the *bit-flip* noise, which is described by the completely positive map

$$\mathcal{E}_1(\rho_0) = \sum_{i,j=0}^{1} E_{ij}\, \rho_0\, E_{ij}^{\dagger}, \tag{20}$$

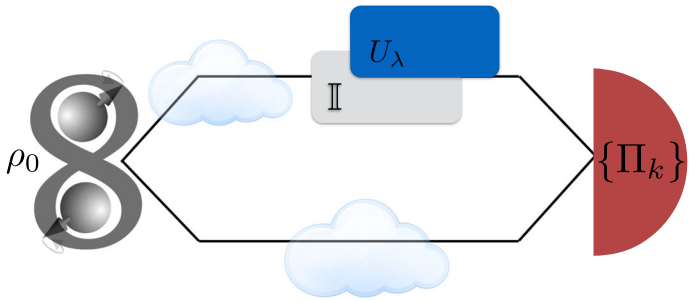

Fig. 3 Process discrimination as a binary decision on noisy entangled state. The signal is subject to some source of noise, which affects both parts of the entangled system, and takes place before the possible perturbation U_λ. At the output, we have a joint detector

where E_{ij} are the Kraus operators:

$$\begin{aligned} E_{00} &= \sqrt{pq}\,\mathbb{I}\otimes\mathbb{I}, \\ E_{01} &= \sqrt{p(1-q)}\,\mathbb{I}\otimes\sigma_1, \\ E_{10} &= \sqrt{(1-p)q}\,\sigma_1\otimes\mathbb{I}, \\ E_{11} &= \sqrt{(1-p)(1-q)}\,\sigma_1\otimes\sigma_1. \end{aligned} \tag{21}$$

In these equations, p and q are the probabilities for, respectively, the first qubit (which has probability to undergo the unitary transformation) and the second qubit to be subject to noise. The probability of occurring noise is assumed as independent on the two channels. If the initial state is $\rho_0 = |\phi_+\rangle\langle\phi_+|$, we get

$$\begin{aligned} \mathcal{E}_1(\rho_0) &= [pq + (1-p)(1-q)]|\phi_+\rangle\langle\phi_+| + [p(1-q) + q(1-p)]|\psi_+\rangle\langle\psi_+| \\ &= (1-p-q+2pq)|\phi_+\rangle\langle\phi_+| + (p+q-2pq)|\psi_+\rangle\langle\psi_+|. \end{aligned} \tag{22}$$

Using Eq. (19), we obtain:

$$p_e = \frac{1}{2}[1 - |(2p-1)(2q-1)||\sin\lambda|]. \tag{23}$$

Similar considerations can be conducted for the *phase-flip* noise by replacing σ_1 in Eq. (21) to σ_3. For the same initial state considered above we get:

$$\mathcal{E}_3(\rho_0) = [pq + (1-p)(1-q)]|\phi_+\rangle\langle\phi_+| + [q(1-p) + p(1-a)]|\phi_-\rangle\langle\phi_-|, \tag{24}$$

and

$$p_e = \frac{1}{2}[1 - |\sin\lambda|]. \tag{25}$$

No dependence on the noise is present, i.e. the discrimination power for the studied protocol is not affected by the presence of phase-flip noise. Analogue results are obtained when discussing the *phase-bit-flip noise*, which is described by the same previous set of Kraus operators by formally replacing σ_1 with σ_2.

Considering as a last case the depolarising noise

$$\mathcal{E}_{\mathrm{dp}}(\rho_0) = \frac{p}{4}\mathbb{I} + (1-p)\rho_0, \tag{26}$$

where p is the probability that the state ρ_0 is transformed to a maximally mixed state $\frac{1}{2}\mathbb{I}$, results of Eq. (19) may be used, leading to

$$p_e = \frac{1}{2}[1 - (1-p)|\sin\lambda|]. \tag{27}$$

As before, this is independent of the mean value of the generator of the perturbation. On the other hand, the probability of error depends on the noise parameter p, and it increases with p. To summarise: when the noise acts on an eigenspace of the perturbation generator, the decision process is affected, and accordingly, the probability of error is increased. On the other hand, when the noise acts on an orthogonal space of the generator of the perturbation U_λ, the probability of error of making a decision results unchanged and it achieves its minimal value given in Eq. (25).

4 Neyman–Pearson strategy and the minimum detectable perturbation

4.1 Pure states

In this section, we address the problem of evaluating the minimum detectable value of the perturbation amplitude λ_{m}, i.e. the minimum value of λ in $U(\lambda) = e^{-i\lambda\sigma_1}$ making ρ_0 and ρ_λ discriminable. To this aim, we have to maximise the detection probability of the alternative hypothesis, which is the basis of the so-called Neyman–Pearson strategy, to optimise binary decision.

We start from a single qubit initially prepared in a pure state. In this case, as it was observed in Sect. 2, the optimal NP strategy may be analytically determined and the characteristic equation $p_{11} = p_{11}(\kappa, p_{10})$ takes the form of the expression shown in Eq. (6), where $\kappa = \langle\psi_0|\psi_\lambda\rangle = \langle\psi_0|U_\lambda|\psi_0\rangle$ is the overlap between the initial and the perturbed states. Given the expression of $U(\lambda) = e^{-i\lambda\sigma_1}$, it is clear that the eigenstates of σ_1 are not modified by the action of the perturbation (up to an irrelevant phase), and thus they are not suitable to detect any value of λ.

In order to define the minimum detectable perturbation, it is necessary to define a criterion to discern the regimes for which the detection probability can be considered large. The first criterion to be employed is an "absolute" one: a perturbation amplitude λ is detectable if it leads to a detection probability $p_{11}(\kappa, p_{10}) \geq \frac{1}{2}$. A lower detection rate would indeed make the dataset useless, as no reliable information may be extracted in that case. We also address a "relative" criterion, for which

a perturbation is considered detectable when it leads to $p_{11}/p_{10} \geq \delta \gg 1$. In order to perform our analysis, we rewrite the expression of $p_{11} = p_{11}(\kappa, p_{10})$ in terms of $\alpha \equiv 1-|\kappa|^2 = (1-r_1^2)\sin^2\lambda$. Concerning the expression of the detection probability, it is clear from Eq. (6) that unit detection probability $p_{11} = 1$ is reached whenever $|\kappa|^2 \leq p_{10}$, i.e. $(1-r_1^2)\sin^2\lambda \geq 1-p_{10}$. In principle, in this regime $p_{11} = 1$ is obtained and thus we may detect arbitrarily small perturbation. However, the condition $|\kappa|^2 \leq p_{10}$ is λ-dependent and this constraint poses a lower bound on the detectable amplitude. This is illustrated in the left panel of Fig. 4, where a contour plot of p_{11} as function of p_{10} and α is shown. The *good* area is the white one above the red straight line $\alpha = 1 - p_{10}$.

The other branch of the function is less trivial to analyse. Nevertheless, it is easy to observe that p_{11} increases with p_{10} and α, and then the $p_{11} \geq \frac{1}{2}$ condition is satisfied in the area between the above-mentioned line and the curve of equation $\left[\sqrt{p_{10}\,(1-\alpha)} + \sqrt{(1-p_{10})\,\alpha}\right]^2 = 1/2, \quad p_{10} \in \left[0, \frac{1}{2}\right]$, which is the red arc of Fig. 4 (both panels). The entire set of couples (p_{10}, α) satisfying the absolute criterion can therefore be graphically represented as the grey-shadowed area in the right panel of Fig. 4. The above equation may be inverted to make α explicit, leading to $\alpha = \frac{1}{2} - \sqrt{p_{10}\,(1-p_{10})}, \quad p_{10} \in \left[0, \frac{1}{2}\right]$. The minimum detectable perturbation can then be calculated upon recalling the expression of α, leading to

$$\lambda_{\mathrm{m}} = \arcsin\sqrt{\frac{1}{1-r_1^2}\left[\frac{1}{2} - \sqrt{p_{10}\,(1-p_{10})}\right]}. \tag{28}$$

In order to make sense of the right-hand side of Eq. (28), the possible values of r_1 must be restricted to $r_1^2 \leq \frac{1}{2} + \sqrt{p_{10}(1-p_{10})}$. This is a limitation on the state construction: if we fix a false-alarm probability $p_{10} \leq \frac{1}{2}$, only states satisfying this condition may lead to a detection probability p_{11} larger than $\frac{1}{2}$. In the rest of our discussion we focus on those states, since for $p_{10} \geq \frac{1}{2}$ we have $p_{11} = 1$, and any state preparations corresponds to an arbitrarily small detectable perturbation. As it was noted above, the optimal preparation of the input signal corresponds to $r_1 = 0$. In this case, varying $p_{10} \in [0, \frac{1}{2}]$, we have $\sin^2\lambda \in [\frac{1}{2}, 0]$. Accepting as instance no false alarm ($p_{10} = 0$), the minimum detectable perturbation parameter is calculated as $\lambda_m = \pi/4$, whereas all the unitary transformations with parameter smaller than $\pi/4$ cannot be detected. When instead the accepted false-alarm probability is fixed to $1/2$ (the largest possible value when considering this branch), all the possible transformation parameters are available: $\lambda_m = 0$. This is yet a relative advantage, because of the trade-off between sensitivity and false-alarm probability. In particular, for values of $p_{10} \simeq \frac{1}{2}$ we have $\lambda_{\mathrm{m}} \simeq \sqrt{\frac{1}{1-r_1^2}\left[\frac{1}{2} - \sqrt{p_{10}\,(1-p_{10})}\right]}$. If r_1 takes its maximum allowed value, that is $r_1^2 = \frac{1}{2} + \sqrt{p_{10}\,(1-p_{10})}$, then $\lambda_{\mathrm{m}} = \pi/2$ independently from the value of the false-alarm probability.

Let us now address the analysis of the second above-mentioned criterion, for which the minimum detectable perturbation leading to $p_{11}/p_{10} \geq \delta \gg 1$ is targeted. As in previous cases, it is easy to address the situation when $\alpha \geq 1 - p_{10}$, for which $p_{11} = 1$. In this case, the criterion may be easily inverted and immediately leads to

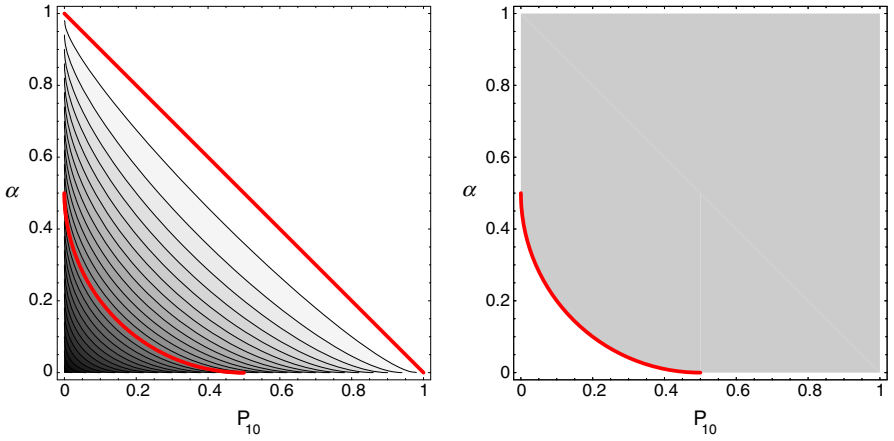

Fig. 4 The minimum detectable perturbation for pure states (absolute criterion). Left panel: contour plot p_{11} as a function of p_{10} and α. Right: the grey area corresponds to the region where $p_{11} \geq \frac{1}{2}$ (Color figure online)

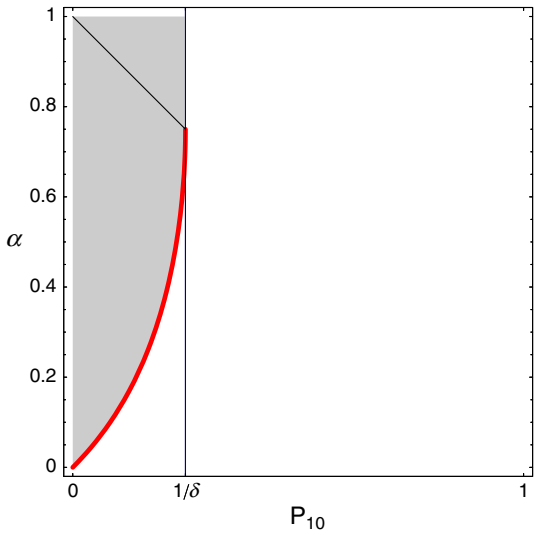

Fig. 5 The minimum detectable perturbation for pure states (relative criterion). The grey area corresponds to the region where $p_{11}/p_{10} \geq \delta$ for the particular case $\delta = 4$

$p_{10} \leq \frac{1}{\delta}$. The corresponding points in the $p_{10} - \alpha$ plane are shown in Fig. 5. In the opposite case ($\alpha \leq 1 - p_{10}$), the inequality $[\sqrt{p_{10}(1-\alpha)} + \sqrt{(1-p_{10})\alpha}]^2 \geq \delta$ has to be solved. After some algebra, we may rewrite this condition as

$$\alpha \geq p_{10}\left[\sqrt{1-\delta p_{10}} - \sqrt{\delta\,(1-p_{10})}\right]^2. \tag{29}$$

The entire area for which the detection probability can be considered large with respect to p_{10} is grey coloured in Fig. 5. Upon increasing δ, the area is decreasing in size, the vertical line moving left.

The minimum detectable perturbation is thus given by

$$\lambda_{\mathrm{m}} = \arcsin \sqrt{\frac{p_{10}}{1-r_1^2}\left[\sqrt{1-\delta p_{10}} - \sqrt{\delta\,(1-p_{10})}\right]^2}, \tag{30}$$

depending on the fixed value of δ and on the state preparation with respect to the σ_1-axis, r_1. The restriction on the possible state preparation reads as follows: $r_1^2 \leq 1 - p_{10}[\sqrt{1-\delta p_{10}} - \sqrt{\delta(1-p_{10})}]^2$.

4.2 Mixed states

Following the same steps for mixed states, we are led to diagonalise the Lagrange characteristic operator $\Gamma = \rho_\lambda - \gamma\rho_0 = \begin{pmatrix} \Gamma_0 & \Gamma_2 \\ \Gamma_2^* & \Gamma_1 \end{pmatrix}$, which is expressed in terms of the Bloch representation of the initial and the perturbed states

$$\Gamma_0 = \frac{1}{2}[(1-\gamma) + (r_{3\lambda} - \gamma r_3)], \tag{31}$$

$$\Gamma_1 = \frac{1}{2}[(1-\gamma) - (r_{3\lambda} - \gamma r_3)], \tag{32}$$

$$\Gamma_2 = \frac{1}{2}[(r_{1\lambda} - \gamma r_1) - i(r_{2\lambda} - \gamma r_2)]. \tag{33}$$

The detection and the false-alarm probabilities are, respectively, given by:

$$p_{11} = \frac{1}{2}\left[1 + \frac{\left(f(\gamma) - \gamma|\kappa|^2\right)\sqrt{r^2}}{\sqrt{f^2(\gamma) - \gamma|\kappa|^2}}\right], \quad p_{10} = \frac{1}{2}\left[1 - \frac{\left(f(\gamma) - |\kappa|^2\right)\sqrt{r^2}}{\sqrt{f^2(\gamma) - \gamma|\kappa|^2}}\right], \tag{34}$$

where $f(\gamma) = \frac{1}{2}(1+\gamma)$ and $|\kappa|^2 = 1 - (1 - \frac{r_1^2}{r^2})\sin^2\lambda$. After careful inspection of the domains of validity, we may invert the above Equations, obtaining the characteristic expression $p_{11} = p_{11}(\kappa, p_{10})$ as follows:

$$p_{11}\,(p_{10}) = \begin{cases} 0 & 0 \leq p_{10}\,(\gamma) \leq p_{10}\,(\gamma_+) \\ p_{11}^* & p_{10}\,(\gamma_+) < p_{10} < p_{10}\,(\gamma_-) \\ p_{11}\,(\gamma_-) & p_{10}\,(\gamma_-) \leq p_{10} \leq 1 \\ 1 & p_{10} = 1 \end{cases}, \tag{35}$$

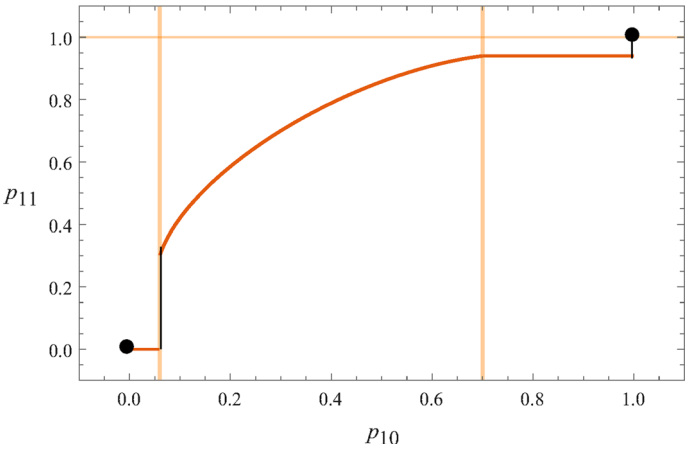

Fig. 6 The minimum detectable perturbation for mixed states. The plot shows the characteristic function of Eq. (35) for an initially mixed state with $r^2 = 0.8$ and $|\kappa|^2 = 0.8$

where $p_{11}^* = p_{10}|\kappa|^2 + (1-p_{10})(1-|\kappa|^2) + \sqrt{|\kappa|^2(1-|\kappa|^2)[r^2-(2p_{10}-1)^2]}$, and the two critical values $\gamma_\pm$ are given by

$$\gamma_\pm = 1 + 2\frac{\sqrt{r^2(1-|\kappa|^2)}}{1-r^2}\left[\sqrt{r^2-|\kappa|^2 r^2} \pm \sqrt{1-|\kappa|^2 r^2}\right]. \tag{36}$$

The characteristic function is graphically represented in Fig. 6 for fixed values of r^2 and κ, which correspond to fix r_1^2 and λ, i.e. to tuning the initial preparation and the setup (remind that $r^2 = 2\mu - 1$, where μ is the purity of the initial preparation). The corresponding minimum detectable perturbation is then given by

$$\lambda_{\mathrm{m}} = \arcsin\sqrt{\frac{1}{1-\frac{r_1^2}{r^2}}\left[\frac{1}{2} - \sqrt{\frac{r^2-1+4p_{10}\,(1-p_{10})}{r^2}}\right]}, \tag{37}$$

with the condition

$$r_1^2 \leq r^2\left[\frac{1}{2} + \sqrt{\frac{r^2-1+4p_{10}\,(1-p_{10})}{r^2}}\right]. \tag{38}$$

Once again, this is a restriction on the initial preparation of the system. When the inequality is saturated, the only parameter that can be detected is $\lambda_m = \frac{\pi}{2}$, otherwise the best preparation is $r_1 = 0$. Of course, λ_m vanishes as far as p_{10} approaches the limiting value $p_{10} = \frac{1}{2}$.

4.3 Pure two-qubit states

Here we address possible enhancement coming from coupling the qubit that might undergo a perturbation U_λ to another qubit which is left unperturbed. We will consider the same setup of the Bayesian analysis, reported in Fig. 2. We obtained before that for a generic pure state described in the computational basis of two qubits by (18) and satisfying $\alpha_0\alpha_2^* + \alpha_1\alpha_3^* = 0$ the overlap has a universal value independent of the preparation; $|\kappa|^2 = \cos^2\lambda$, and thus $\alpha = \sin^2\lambda$. If we compare this result with what we found in the case of generic single-qubit state, we see that they match up whenever the state is pure and the projection on the generator axis vanishes. The corresponding minimum detectable perturbation is given by

$$\lambda_{\rm m} = \arcsin\sqrt{\frac{1}{2} - \sqrt{p_{10}\,(1-p_{10})}}, \tag{39}$$

which does not depend on the initial preparation of the system and ranges from 0 to $\frac{\pi}{4}$ for p_{10} ranging from $\frac{1}{2}$ to 0. As we already concluded for the Bayesian case, the effect of entanglement is to enhance the overall stability of the discrimination/estimation scheme.

4.4 Mixed two-qubit states

Let us consider here a generic Bell-diagonal mixed state $\rho_0 = p_0\,|\phi_+\rangle\langle\phi_+| + p_1\,|\psi_+\rangle\langle\psi_+| + p_2\,|\psi_-\rangle\langle\psi_-| + p_3\,|\phi_-\rangle\langle\phi_-|$, $\sum_k p_k = 1$. The Lagrange operator $\Gamma = \rho_\lambda - \gamma\rho_0$ for this preparation may be decomposed into a direct sum of two operators, each one acting on the orthogonal subspaces generated by $\{|\phi_+\rangle, |\psi_+\rangle\}$ and $\{|\phi_-\rangle, |\psi_-\rangle\}$, respectively. In particular, we have

$$\mathbf{\Gamma} = \mathbf{\Gamma}^{(+)} \oplus \mathbf{\Gamma}^{(-)}, \tag{40}$$

where

$$\begin{aligned}\mathbf{\Gamma}^{(+)} = &\left[p_0(\cos^2\lambda - \gamma) + p_1\sin^2\lambda\right]|\phi_+\rangle\langle\phi_+| \\ &+ \left[p_1(\cos^2\lambda - \gamma) + p_0\sin^2\lambda\right]|\psi_+\rangle\langle\psi_+| \\ &+ i\,\sin\lambda\cos\lambda(p_0 - p_1)\,(|\phi_+\rangle\langle\psi_+| - |\psi_+\rangle\langle\phi_+|)\,,\end{aligned} \tag{41}$$

and

$$\begin{aligned}\mathbf{\Gamma}^{(-)} = &\left[p_2(\cos^2\lambda - \gamma) + p_3\sin^2\lambda\right]|\phi_-\rangle\langle\phi_-| \\ &+ \left[p_3(\cos^2\lambda - \gamma) + p_2\sin^2\lambda\right]|\psi_-\rangle\langle\psi_-| \\ &+ i\,\sin\lambda\cos\lambda\,(p_2 - p_3)\,(|\phi_-\rangle\langle\psi_-| - |\psi_-\rangle\langle\phi_-|)\,.\end{aligned} \tag{42}$$

The two operators may be brought to a 2×2 matrix form as

$$\mathbf{\Gamma}^{(\pm)} = \begin{pmatrix} \Gamma_0^{(\pm)} & \Gamma_2^{(\pm)} \\ (\Gamma_2^{(\pm)})^* & \Gamma_1^{(\pm)} \end{pmatrix}, \tag{43}$$

with

$$\begin{aligned} \Gamma_0^{(+)} &= p_0(\cos^2\lambda - \gamma) + p_1 \sin^2\lambda, & \Gamma_0^{(-)} &= p_2(\cos^2\lambda - \gamma) + p_3 \sin^2\lambda, \\ \Gamma_1^{(+)} &= p_1(\cos^2\lambda - \gamma) + p_0 \sin^2\lambda, & \Gamma_1^{(-)} &= p_3(\cos^2\lambda - \gamma) + p_2 \sin^2\lambda, \\ \Gamma_2^{(+)} &= i\ \sin\lambda\cos\lambda(p_0 - p_1), & \Gamma_2^{(-)} &= i \sin\lambda\cos\lambda(p_2 - p_3). \end{aligned} \tag{44}$$

For the sake of clarity, let us discuss explicitly how to derive the characteristic function. The relevant quantities for discussing the eigenvalues of $\mathbf{\Gamma}$ are trace and determinant of $\mathbf{\Gamma}^{(\pm)}$. We have

$$\mathrm{Tr}[\mathbf{\Gamma}^{(+)}] = (p_0 + p_1)(1 - \gamma) \tag{45}$$

$$\det \mathbf{\Gamma}^{(+)} = p_0 p_1[\gamma^2 - 2\gamma(1 + \Xi^{(+)}) + 1], \tag{46}$$

where

$$\Xi^{(+)} = \frac{(p_0 - p_1)^2}{2p_0 p_1}\sin^2\lambda. \tag{47}$$

The two critical values of γ, corresponding to vanishing determinant, are

$$\gamma_\pm^{(+)} = 1 + \Xi^{(+)} \pm \sqrt{\Xi^{(+)}\left(\Xi^{(+)} + 2\right)}. \tag{48}$$

Accordingly, three regimes are identified, summarised as follows:

$$\begin{cases} \gamma^{(+)} \leq \gamma_-^{(+)}, \ \ \zeta_\pm \geq 0 & \Pi = \{\Pi_0 = \mathbb{O}, \Pi_1 = \mathbb{I}_4\} \\ \gamma^{(+)} \geq \gamma_+^{(+)}, \ \ \zeta_\pm \leq 0 & \Pi = \{\Pi_0 = \mathbb{I}_4, \Pi_1 = \mathbb{O}\} \\ \gamma_-^{(+)} < \gamma^{(+)} < \gamma_+^{(+)}, \ \ \zeta_- \leq 0;\ \zeta_+ > 0 & \Pi = \{\Pi_0 = |\zeta_-\rangle\langle\zeta_-|\,, \Pi_1 = |\zeta_+\rangle\langle\zeta_+|\} \end{cases} \tag{49}$$

where $\zeta_\pm$ are the eigenvalues of the operator $\mathbf{\Gamma}^{(+)}$. Upon carrying out the same analysis for $\mathbf{\Gamma}^{(-)}$, we identify the critical values for the Lagrange multiplier. Depending on the initial parameters $\{p_i\}_{i=0,1,2,3}$, the intervals $[\gamma_-^{(-)}, \gamma_+^{(-)}]$ and $[\gamma_-^{(+)}, \gamma_+^{(+)}]$ are contained one in the other. Focusing on the case $\Xi^{(+)} \geq \Xi^{(-)}$, it is observed that $[\gamma_-^{(-)}, \gamma_+^{(-)}] \subseteq [\gamma_-^{(+)}, \gamma_+^{(+)}]$. The characteristic function may then be explicitly parameterised by γ as follows:

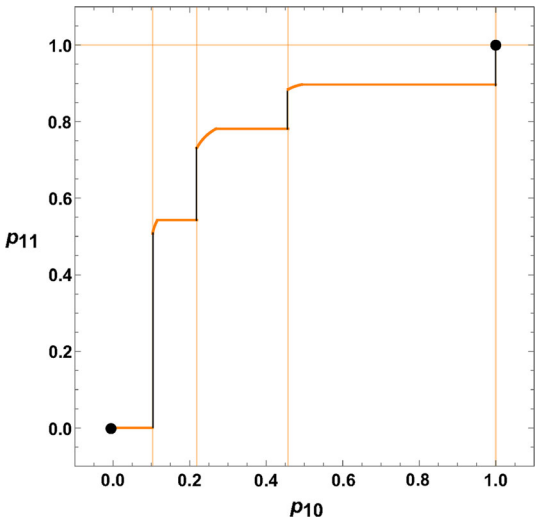

Fig. 7 The characteristic function of Eq. (50) for a diagonal mixed state with coefficients $p_0 = 0.1$, $p_1 = 0.2$, $p_2 = 0.1$ and $p_3 = 0.6$

$$
\begin{cases}
p_{10} = 1 & p_{11} = 1 \\
p_{10} = \frac{1}{2}\left[(p_0 + p_1) + |p_0 - p_1| \times \frac{\cos 2\lambda - \gamma}{\sqrt{\gamma^2 - 2\gamma\cos 2\lambda + 1}}\right] + (p_2 + p_3) & p_{11} = \frac{1}{2}\left[(p_0 + p_1) + |p_0 - p_1| \times \frac{1 - \gamma\cos 2\lambda}{\sqrt{\gamma^2 - 2\gamma\cos 2\lambda + 1}}\right] + (p_2 + p_3) \\
p_{10} = \frac{1}{2}\left[1 + (|p_2 - p_3| + |p_0 - p_1|) \times \frac{\cos 2\lambda - \gamma}{\sqrt{\gamma^2 - 2\gamma\cos 2\lambda + 1}}\right] & p_{11} = \frac{1}{2}\left[1 + (|p_2 - p_3| + |p_0 - p_1|) \times \frac{1 - \gamma\cos 2\lambda}{\sqrt{\gamma^2 - 2\gamma\cos 2\lambda + 1}}\right] \\
p_{10} = \frac{1}{2}\left[(p_0 + p_1) + |p_0 - p_1| \times \frac{\cos 2\lambda - \gamma}{\sqrt{\gamma^2 - 2\gamma\cos 2\lambda + 1}}\right] & p_{11} = \frac{1}{2}\left[(p_0 + p_1) + |p_0 - p_1| \times \frac{1 - \gamma\cos 2\lambda}{\sqrt{\gamma^2 - 2\gamma\cos 2\lambda + 1}}\right] \\
p_{10} = 0 & p_{11} = 0
\end{cases}
\tag{50}
$$

An example of this characteristic function with a particular choice of the preparation parameters p_0, p_1, p_2, p_3 and the perturbation parameter λ is illustrated in Fig. 7. Similar calculations can be conducted in the other case for which: $\Xi^{(-)} \geq \Xi^{(+)}$.

Using arguments similar to those developed in this section, we may deal with discrimination in the presence of noise and find the minimum detectable perturbation also in those cases. Finally, we notice that the use of entanglement can positively affect the discrimination process of quantum states by confirming the overall precision obtained in the single-qubit protocol, while enhancing the stability of the detection scheme by removing the dependence on the preparation of the initial state.

5 Conclusions

In this paper, we have applied concepts and methods from quantum decision theory to address process discrimination and estimation in qubit systems. In particular, we have discussed the problem of discriminating whether or not a given unitary perturbation was applied to a qubit system, as well as the complementary problem of evaluating the minimum detectable perturbation amplitude leading to discriminable outputs. Our approach has allowed us to obtain several results which are summarised in the following.

We have seen that entanglement may represent a resource, in particular for improving the stability of the discrimination strategies. Using single-qubit pure probes, the characteristic function for both Bayes and NP strategy does explicitly depend on the initial preparation, whereas using two-qubit probes this dependence disappears. Bell-state probes are shown to be optimal for both strategies. Nevertheless, they are not the only choice, since there exists an entire class of states, depending on the generator of the unitary perturbation, for which both strategies are optimised. In this sense, it has been shown that not only Bell states belong to this class, but there exists also a set of non-balanced states simultaneously optimal for each generator.

A similar analysis has been performed for single- and two-qubit mixed states, for which we found novel analytic solutions for Bayes error probability and the NP characteristic function. In this way, we found that optimal preparations correspond to pure states with a vanishing value of the generator expectation value. We have then used our results to explicitly discuss the effects of possible background noises on the discrimination performance of the various strategies and schemes. Overall, besides the exact quantification of noise effects, we have the rather intuitive conclusion that when we bring noise into play, it has detrimental effects only when it acts on the eigenspaces of the generator, whereas it has no effects when acting on orthogonal subspaces.

Acknowledgements MGAP is member of GNFM-INdAM.

References

1. Yuen, H.P., Kennedy, R.S., Lax, M.: Optimum testing of multiple hypotheses in quantum detection theory. IEEE Trans. Inf. Theory **IT21**, 125 (1975)
2. Helstrom, C.W.: Detection theory and quantum mechanics I. Inform. Control **10**, 254 (1967)
3. Helstrom, C.W.: Detection theory and quantum mechanics II. Inform. Control **13**, 156 (1968)
4. Helstrom, C.W.: Quantum Detection and Estimation Theory. Academic Press, New York (1976)
5. Ivanovic, I.D.: How to differentiate between non-orthogonal states. Phys. Lett. A **123**, 257 (1987)
6. Dieks, D.: How to differentiate between non-orthogonal states. Phys. Lett. A **126**, 303 (1988)
7. Peres, A.: How to differentiate between non-orthogonal states. Phys. Lett. A **128**, 19 (1988)
8. Bergou, J.A., Herzog, U., Hillery, M.: Discrimination of quantum states. Lect. Notes Phys. **649**, 415 (2004)
9. Chefles, A.: Quantum states: discrimination and classical information transmission: a review of experimental progress. Lect. Notes Phys. **649**, 465 (2004)
10. Tomassoni, N., Paris, M.G.A.: Quantum binary channels with mixed states. Phys. Lett. A **373**, 61 (2008)
11. Bergou, J.A.: Discrimination of quantum states. J. Mod. Opt. **57**, 160 (2010)
12. Barnett, S.M., Chefles, A., Jex, I.: Comparison of two unknown pure quantum states. Phys. Lett. A **307**, 189 (2003)

13. Jex, I., Andersson, E., Chefles, A.: Comparing the states of many quantum systems. J. Mod. Opt. **51**, 505 (2004)
14. Andersson, E., Curty, M., Jex, I.: Experimentally realizable quantum comparison of coherent states and its applications. Phys. Rev. A **74**, 022304 (2006)
15. Bennett, C.H.: Quantum cryptography using any two nonorthogonal states. Phys. Rev. Lett. **68**, 3121 (1992)
16. Ekert, A.K.: Quantum cryptography based on Bell's theorem. Phys. Rev. Lett. **67**, 661 (1991)
17. Goldenberg, L., Vaidman, L.: Quantum cryptography based on orthogonal states. Phys. Rev. Lett. **75**, 1239 (1995)
18. Guo, G.-C., Shi, B.-S.: Quantum cryptography based on interaction-free measurement. Phys. Lett. A **256**, 109 (1999)
19. Paris, M.G.A.: Optical qubit by conditional interferometry. Phys. Rev. A **62**, 033813 (2000)
20. Lucamarini, M., Mancini, S.: Secure deterministic communication without entanglement. Phys. Rev. Lett. **94**, 140501 (2005)
21. Bennett, C.H., Brassard, G.: Quantum cryptography: public key distribution and coin tossing. Theor. Comput. Sci. **560**, 7 (2014)
22. Scarani, V., Kurtsiefer, C.: The black paper of quantum cryptography: real implementation problems. Theor. Comput. Sci. **560**, 27 (2014)
23. Avella, A., et al.: Experimental quantum-cryptography scheme based on orthogonal states. Phys. Rev. A **82**, 062309 (2010)
24. Brida, G., et al.: Experimental realization of counterfactual quantum cryptography. Laser Phys. Lett. **9**, 247 (2012)
25. Kimura, G., Miyadera, T., Imai, H.: Optimal state discrimination in general probabilistic theories. Phys. Rev. A **79**, 062306 (2009)
26. Jafarizadeh, M.A., Mazhari, Y., Aali, M.: The minimum-error discrimination via Helstrom family of ensembles and convex optimization. Quantum Inf. Proc. **10**, 155 (2011)
27. Jafarizadeh, M.A., Mazhari Khiavi, Y., Akbari Kourbolagh, Y.: Minimum-error discrimination between two sets of similarity-transformed quantum states. Quantum Inf. Proc. **12**, 2835 (2013)
28. D'Ariano, G.M., Lo Presti, P., Paris, M.G.A.: Improved discrimination of unitary transformations by entangled probes. J. Opt. B **4**, S273 (2002)
29. Laing, A., Rudolph, T., O'Brien, J.L.: Experimental quantum process discrimination. Phys. Rev. Lett. **102**, 160502 (2009)
30. Invernizzi, C., Paris, M.G.A.: The discrimination problem for two ground states or two thermal states of the quantum Ising model. J. Mod. Opt. **57**, 198 (2010)
31. Deville, Y., Deville, A.: Classical-processing and quantum-processing signal separation methods for qubit uncoupling. Quantum Inf. Proc. **11**, 1311 (2012)
32. Wittek, P.: Quantum Machine Learning, p. 125. Academic Press, New York (2014)
33. Bae, J., Kwek, L.-C.: Quantum state discrimination and its applications. J. Phys. A **48**, 083001 (2015)
34. Trapani, J., Paris, M.G.A.: Entanglement as a resource for discrimination of classical environments. Phys. Lett. A **381**, 245 (2017)
35. Rehman, J., Farooq, A., Jeong, Y., Shin, H.: Quantum channel discrimination without entanglement. Quantum Inf. Proc. **17**, 271 (2018)
36. Chesi, G., Olivares, S., Paris, M.G.A.: Squeezing-enhanced phase-shift-keyed binary communication in noisy channels. Phys. Rev. A **97**, 032315 (2018)
37. Takeoka, M., Ban, M., Sasaki, M.: Practical scheme for optimal measurement in quantum interferometric devices. Phys. Lett. A **313**, 16 (2003)
38. Paris, M.G.A.: Interferometry as a binary decision problem. Phys. Lett. A **225**, 23 (1997)
39. Ralph, J.F., Clark, T.D., Prance, R.J., Prance, H.: A likelihood ratio test applied to a radio-frequency SQUID Hamiltonian. Phys. Lett. A **277**, 75 (2000)
40. Duan, R., Feng, Y., Ying, M.: Local distinguishability of multipartite unitary operations. Phys. Rev. Lett. **100**, 020503 (2008)
41. Cao, T.-Q., Gao, F., Yang, Y.-H., Zhang, Z.-C., Wen, Q.-Y.: Determination of locally perfect discrimination for two-qubit unitary operations. Quantum Inf. Proc. **15**, 529 (2016)